Developmental Cell, Vol. 6, 423–435, March, 2004, Copyright ©2004 by Cell Press

# A Twist Code Determines the Onset of Osteoblast Differentiation

**Peter Bialek,[1,6] Britt Kern,[1,2,6] Xiangli Yang,[1] Marijke Schrock,[1] Drazen Sosic,[3] Nancy Hong,[4] Hua Wu,[4] Kai Yu,[5] David M. Ornitz,[5] Eric N. Olson,[3] Monica J. Justice,[1] and Gerard Karsenty[1,*]**
[1]Department of Molecular and Human Genetics
Bone Disease Program of Texas
[2]Interdepartmental Program of Cell and Molecular Biology
Baylor College of Medicine
One Baylor Plaza
Houston, Texas 77030
[3]Department of Molecular Biology
University of Texas Southwestern Medical Center
6000 Harry Hines Boulevard
Dallas, Texas 75390
[4]Phenomix Corporation
11099 North Torrey Pines Road
La Jolla, California 92037
[5]Department of Molecular Biology and Pharmacology
Washington University Medical School
660 South Euclid Avenue
St. Louis, Missouri 63110

## Summary

**Runx2 is necessary and sufficient for osteoblast differentiation, yet its expression precedes the appearance of osteoblasts by 4 days. Here we show that Twist proteins transiently inhibit Runx2 function during skeletogenesis. *Twist-1* and *-2* are expressed in *Runx2*-expressing cells throughout the skeleton early during development, and osteoblast-specific gene expression occurs only after their expression decreases. Double heterozygotes for *Twist-1* and *Runx2* deletion have none of the skull abnormalities observed in *Runx2*$^{+/-}$ mice, a *Twist-2* null background rescues the clavicle phenotype of *Runx2*$^{+/-}$ mice, and *Twist-1* or *-2* deficiency leads to premature osteoblast differentiation. Furthermore, *Twist-1* overexpression inhibits osteoblast differentiation without affecting *Runx2* expression. Twist proteins' antiosteogenic function is mediated by a novel domain, the Twist box, which interacts with the Runx2 DNA binding domain to inhibit its function. In vivo mutagenesis confirms the antiosteogenic function of the Twist box. Thus, relief of inhibition by Twist proteins is a mandatory event precluding osteoblast differentiation.**

## Introduction

Molecular understanding of osteoblast differentiation has made major progress in the last few years with the identification of genes regulating it specifically (Karsenty and Wagner, 2002). Among them, *Runx2* (formerly *Cbfa1*), a cell-specific member of the *Runx* family of transcription factors, plays a pivotal role. *Runx2* is the earliest and most specific molecular marker of the osteoblast lineage, its expression is both necessary and sufficient to induce osteoblast differentiation, and it regulates expression of most genes characteristic of the osteoblast phenotype (Ducy et al., 1997; Komori et al., 1997; Otto et al., 1997). *Runx2* is also required for chondrocyte hypertrophy in bones ossifying through endochondral ossification (Takeda et al., 2001; Ueta et al., 2001).

*Runx2* expression is detected in lateral plate mesoderm as early as E10 during mouse development (Ducy, 2000), yet expression of molecular markers of differentiated osteoblasts cannot be detected before E13 at the earliest, and in most skeletal elements, replacement of the cartilaginous template by bone does not occur before E15 (Bianco et al., 1991; Chen et al., 1992; Kaufman et al., 1992). This delay between *Runx2* expression and osteoblast differentiation implies that other regulatory proteins are involved in this process. Conceivably, these other regulatory proteins could belong to one of two classes of molecules. Some could be activators of transcription whose expression is controlled by *Runx2*. Osterix, an osteoblast-specific zinc-finger protein, is such a molecule (Nakashima et al., 2002). Others could be inhibitors of Runx2 function that would be expressed transiently in osteoblast progenitors. Consistent with the hypothesis that osteoblast differentiation may be negatively regulated, some skeletal dysplasias are characterized by an increased bone formation (Mundlos and Olsen, 1997).

Twist proteins are basic helix-loop-helix (bHLH)-containing transcription factors. Two *Twist* genes exist in vertebrates, *Twist-1* and *-2* (formerly *dermo-1*) (Wolf et al., 1991; Li et al., 1995). Gene deletion experiments have shown that *Twist-1* is required for closure of the neural tube during mouse development (Chen and Behringer, 1995), while mice homozygous for a *Twist-2* null allele show elevated expression of proinflammatory cytokines causing perinatal death. Twist-1 and -2 repress cytokine gene expression by inhibiting RelA transactivation function through an undefined mechanism (Sosic et al., 2003). Additionally, *Twist-1*$^{+/-}$ mice present a craniosynostosis phenotype such as an increased bone formation in cranial sutures. The same is true in Saethre-Chotzen patients (El Ghouzzi et al., 1997; Howard et al., 1997) who are heterozygous for *Twist-1* inactivation. This latter observation raises the hypothesis that Twist-1 and possibly Twist-2 could inhibit osteoblast differentiation by inhibiting Runx2 function.

Here we show that Twist proteins transiently inhibit osteoblast differentiation during skeletogenesis through the interaction of a novel domain in these proteins and Runx2 DNA binding domain. These results reveal an unanticipated complexity in osteoblast differentiation whose initiation is determined by the relief of an inhibition.

*Correspondence: karsenty@bcm.tmc.edu
[6]These authors contributed equally to this work.

## Results

### Comparison of *Twist-1, -2*, and *Runx2* Expression during Osteoblast Differentiation

To ascertain whether *Twist-1* expression in the developing skeleton was compatible with a role as an inhibitor of osteoblast differentiation, we performed in situ hybridization analysis comparing expression of *Twist-1*, *Runx2*, and *Bone sialoprotein* (*Bsp*), a marker of differentiated osteoblasts (Bianco et al., 1991; Chen et al., 1992) (Figure 1). Given the craniosynostosis phenotype of the *Twist-1*$^{+/-}$ mice, we focused this analysis on the developing skull. At E12, *Runx2* was expressed in cells of the future temporal and parietal bones but not in any other cells of the developing skull (Figure 1A). In contrast, *Twist-1* was strongly expressed in *Runx2*-expressing cells of the presumptive temporal and parietal bones and also in cells of the future frontal and occipital bones where *Runx2* was not yet expressed (Figure 1B). At that stage, *Bsp* expression could not be detected (Figure 1C). At E13, *Runx2* expression had increased in intensity in cells of the temporal and parietal bones and was also detectable in cells of the future occipital bone, while *Twist-1* expression was still high in most cells of the presumptive skull. *Bsp* was expressed in a small area of the temporal bone in cells expressing *Runx2* but not *Twist-1* (Figure 1, compare 1D–1F). At E14, *Runx2* was highly expressed in cells of the future temporal, parietal, and occipital bones (Figure 1G), while *Twist-1* expression was now of weaker intensity throughout the skull (Figure 1H). Following this decrease in *Twist-1* expression, *Bsp* expression was detected in all *Runx2*-expressing cells of the temporal and parietal bones (Figure 1I). A higher magnification analysis showed that *Bsp*-expressing cells expressed *Runx2* but not *Twist-1* (Figures 1J–1L). At E15, *Runx2* expression had become stronger and broader, while *Twist-1* expression was now markedly decreased (Figures 1M and 1N). *Bsp* expression was higher in cells of the parietal and temporal bones in which *Twist-1* expression was low and *Runx2* expression high (Figures 1M–1O).

The similarity of sequence between *Twist-1* and *-2* prompted us to compare *Twist-2*, *Runx*, and *Bsp* expression in the developing skeleton. At E12 and E13, *Twist-2* was coexpressed with *Runx2* in cells of the developing fore- and hindlimbs, the ribs, and vertebrae (Figures 1P and 1Q and data not shown). At that stage, we could not detect *Bsp* expression in any of these skeletal elements (Figure 1R and data not shown). In contrast, at E14, *Twist-2* expression has disappeared in *Runx2*-expressing cells of the forelimbs, ribs, and vertebrae where *Bsp* expression was now detected, indicating that osteoblast differentiation has occurred (Figures 1S–1U and data not shown). Taken together, these data suggest that osteoblast differentiation occurs only after *Twist* gene expression decreases.

### Genetic Interaction between *Twists* and *Runx2*

To assess if there was a genetic interaction between Twist genes and *Runx2*, we generated mice heterozygous for both *Twist-1* and *Runx2* inactivation or homozygous for Twist-2 inactivation and heterozygous for Runx2 inactivation and analyzed their skeletal phenotypes using alcian blue/alizarin red staining of skeletal preparations. *Runx2*$^{+/-}$ mice have delayed closure of the fontanelles due to a delay in osteoblast differentiation (Otto et al., 1997), whereas *Twist-1*$^{+/-}$ mice have larger intraparietal bones and premature fusion of the coronal sutures (Figure 2A) (El Ghouzzi et al., 1997; Howard et al., 1997). In contrast, mice heterozygous for *Twist-1* and *Runx2* inactivation have a normally shaped skull, intraparietal bones of nearly normal size, and no premature fusion of their coronal sutures (Figures 2A and 2B). These observations reveal a genetic interaction between *Twist-1* and *Runx2* during development of the skull, a part of the skeleton whose ossification does not require chondrogenesis. There was no rescue of the hypoplastic clavicle phenotype, another feature of *Runx2*$^{+/-}$ mice, indicating that *Twist-1* alone does not affect osteoblast differentiation in this skeletal element (Figure 2A).

*Twist-2* haploinsufficiency did not correct the skeletal abnormalities of *Runx2*$^{+/-}$ mice, while mice homozygous for *Twist-2* deletion and heterozygous for *Runx2* inactivation ($n = 6$) had a near-complete rescue of the clavicle hypoplasia characteristic of *Runx2*$^{+/-}$ mice (Otto et al., 1997) (Figure 2C). These mice were analyzed at birth, since the *Twist-2* mutation is lethal thereafter (Sosic et al., 2003). *Twist-2* deletion did not affect the skull abnormalities observed in *Runx2*$^{+/-}$ mice, and this is consistent with the fact that *Twist-2* and *Runx2* are not coexpressed in the developing skull (data not shown).

### Premature Osteoblast Differentiation in Absence of *Twists*' Expression

The pattern of *Twist-1* and *-2* expression during osteoblast differentiation and the rescue of the *Runx2* haploinsufficiency phenotype by *Twists*' inactivation support the hypothesis that *Twist-1* and *-2* inhibit osteoblast differentiation. To determine if that is the case, we analyzed skulls of *Twist-1*$^{+/-}$ embryos using mineralized trabeculae and *Osteocalcin*-expressing cells as indicators of differentiated osteoblasts in this structure ossifying through an intramembranous process. In E15 embryos, there were virtually no mineralized trabeculae in wild-type (wt) future parietal bone. In contrast, they were already present in *Twist-1*$^{+/-}$ parietal bones and extended toward the midline (Figures 3Ba and 3Bb). *Osteocalcin* was not expressed in E15 wt parietal bone at that stage, while it was already detectable in *Twist-1*$^{+/-}$ parietal bone and extended toward the midline (Figures 3Be and 3Bf). At E16, mineralized trabeculae were present in both wt and *Twist-1*$^{+/-}$ parietal bones; however, they extended significantly further toward the midline in *Twist-1*$^{+/-}$ than in wt parietal bones (Figures 3Bc and 3Bd). There was expression of *Osteocalcin* in a small area of the wt parietal bones, while the zone of *Osteocalcin*-expressing cells extended further toward the midline in *Twist-1*$^{+/-}$ embryos (Figure 3Bg and 3Bh). At P2, mineralized trabeculae had now reached the midline suture in *Twist-1*$^{+/-}$ but not in wt skulls (Figures 3Ca and 3Cb). Likewise, *Osteocalcin* expression could be detected on both sides of the suture and reached the midline in P2 *Twist-1*$^{+/-}$ but not in wt skulls (Figures 3Cc and

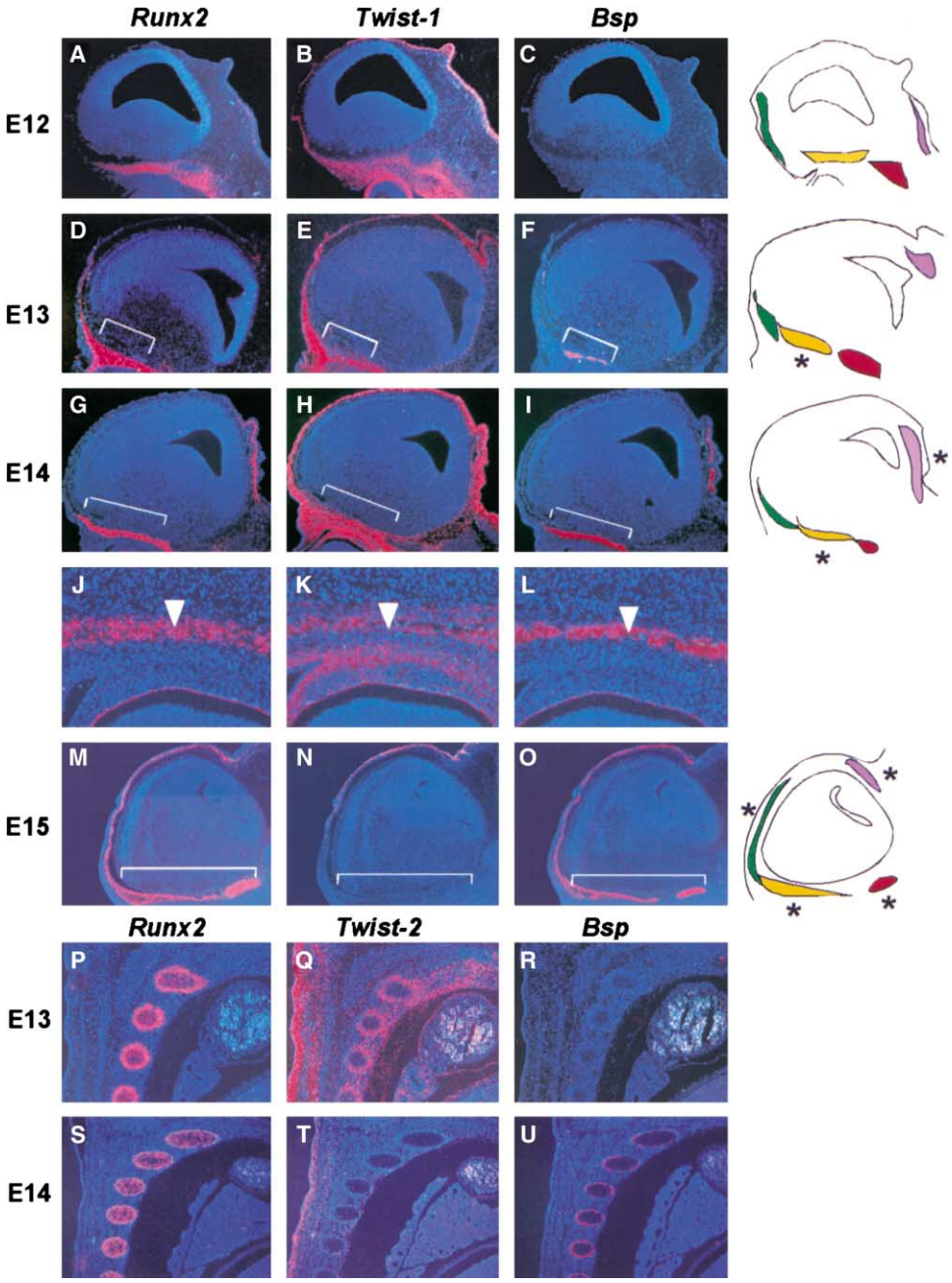


Figure 1. *Twist-1* and *Twist-2* Expression during Osteoblast Differentiation

(A–O) In situ hybridization for *Twist-1*, *Runx2*, and *Bsp* during skull development. Adjacent sections of heads of E12 (A–C), E13 (D–F), E14 (G–L), and E15 (M–O) embryos were hybridized with *Runx2* (A, D, G, J, and M), *Twist-1* (B, E, H, K, and N), or *Bsp* (C, F, I, L, and O) probes. As *Twist-1* expression declines in the developing bones of the skull, *Bsp* expression becomes detectable. Brackets indicate the regions within the parietal and temporal bones expressing *Bsp*. Arrows within the higher magnification of E14 skulls indicate areas expressing *Runx2* and *Bsp* but not *Twist-1*. On the right, schematic representation of skulls at each time point indicates the developing bones as follows: green, frontal; yellow, parietal; red, temporal; and purple, occipital. Asterisks mark areas with detectable *Bsp* expression. (P–U) Analysis of *Runx2*, *Twist-2*, and *Bsp* expression during development. Adjacent sections of ribs (P–U) at E13 (P–R and V–X) and at E14 (S–U and Y–AA). *Bsp* expression is only detected in the ribs once *Twist-2* expression disappears. Magnification: 50-fold, (A)–(I) and (P)–(U); 200-fold, (J)–(L); and 25-fold, (M)–(O).

3Cd). These findings and the expression pattern of *Osteocalcin* in wt and *Twist-1*$^{+/-}$ developing frontal bones (see Supplemental Figure S1A at http://www.developmentalcell.com/cgi/content/full/6/3/423/DC1) indicate that *Twist-1*$^{+/-}$ haploinsufficiency results in premature osteoblast differentiation in the skull, which in turn leads to premature suture closure.

We also analyzed E14 wt and *Twist-2* null embryos.

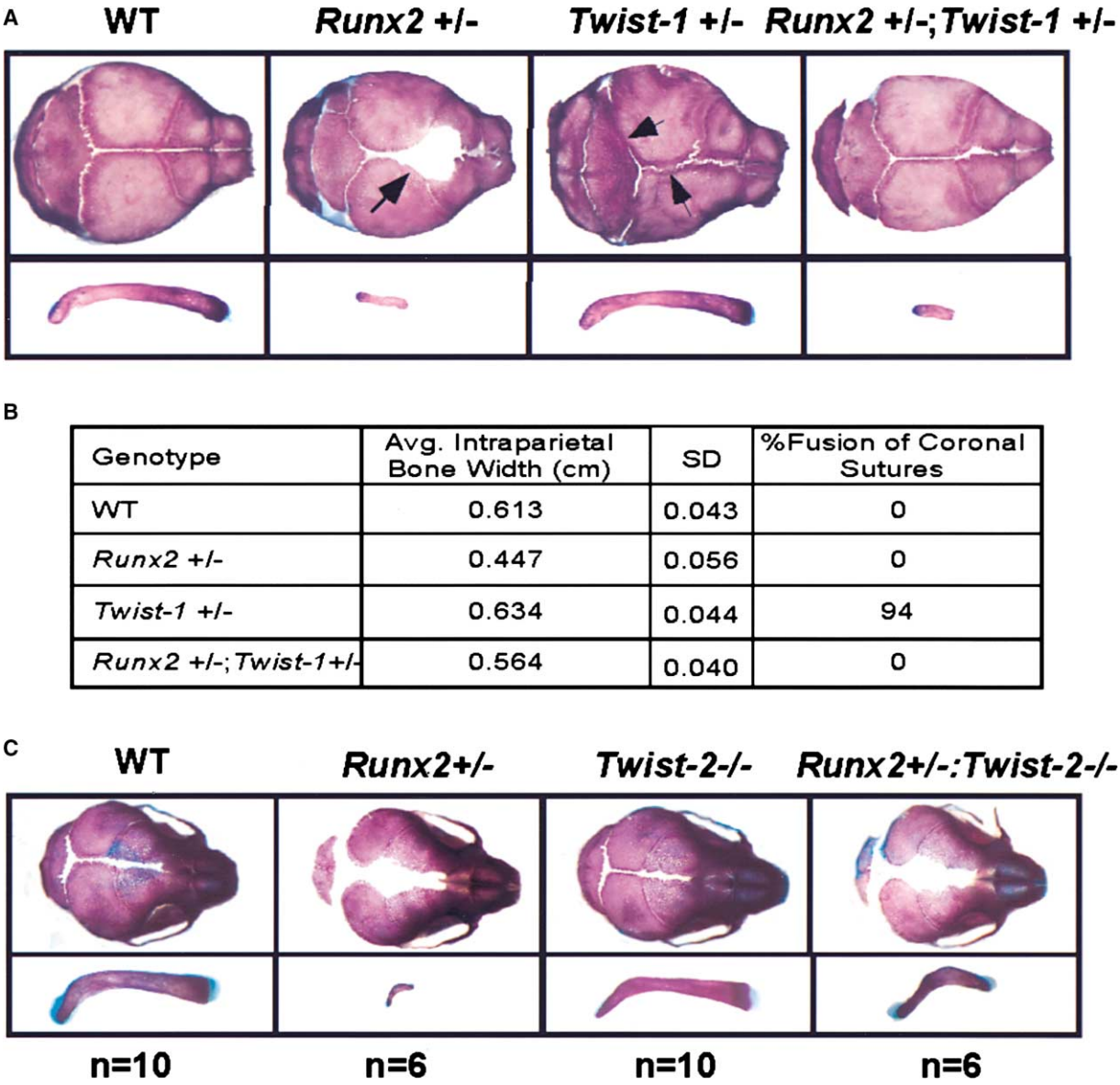


| Genotype | Avg. Intraparietal Bone Width (cm) | SD | %Fusion of Coronal Sutures |
|---|---|---|---|
| WT | 0.613 | 0.043 | 0 |
| *Runx2 +/-* | 0.447 | 0.056 | 0 |
| *Twist-1 +/-* | 0.634 | 0.044 | 94 |
| *Runx2 +/-;Twist-1+/-* | 0.564 | 0.040 | 0 |

Figure 2. *Twist-1* and *-2* Interact Genetically with *Runx2*

(A) Alizarin red/alcian blue-stained preparations of the skull and clavicles from 10-day-old wt, *Runx2*$^{+/-}$, *Twist-1*$^{+/-}$, and *Runx2*$^{+/-}$; *Twist-1*$^{+/-}$ mice. *Runx2*$^{+/-}$ mice display a delay in closure of the fontanelles (arrows) and a decrease in the size of the intraparietal bone and hypoplastic clavicles. *Twist-1*$^{+/-}$ mice display craniosynostosis, that is, increased growth of several bones and fusion of the coronal sutures (arrows). Mice heterozygous for both *Runx2* and *Twist-1* deletions have a normal skull. *Twist-1* haploinsufficiency does not rescue the clavicle hypoplasia of *Runx2*$^{+/-}$ mice.

(B) Width of the intraparietal bones and the percentage of mice with fused coronal sutures in 10-day-old wt, *Runx2*$^{+/-}$, *Twist-1*$^{+/-}$, and *Runx2*$^{+/-}$; *Twist-1*$^{+/-}$ mice. In *Runx2*$^{+/-}$; *Twist-1*$^{+/-}$ mice, the intraparietal bone was close to normal size, and the coronal suture phenotype of *Twist-1*$^{+/-}$ mice was completely rescued ($p < 0.02$ for all parameters).

(C) Alizarin red/alcian blue-stained preparations of skulls and clavicles from newborn pups wt, *Runx2*$^{+/-}$, *Twist-2*$^{-/-}$, and *Runx2*$^{+/-}$; *Twist-2*$^{-/-}$ mice. Note the rescue of the hypoplastic clavicle in *Runx2*$^{+/-}$; *Twist-2*$^{-/-}$ mice, while the skull abnormalities of *Runx2*$^{+/-}$ mice were not corrected.

*Osteocalcin* expression was undetectable in the E14 wt skeletal elements examined but was present in cells of the developing ribs and clavicles of *Twist-2* null embryos ($n = 3$) (Figures 3Da–3Dd). Consistent with this pattern of *Osteocalcin* expression, histological analysis of adjacent sections showed typical cuboidal osteoblasts organized in bone collar-like structures around developing ribs in E14 *Twist2* null but not in wt embryos. Furthermore, there was evidence of vascular invasion, as shown by the presence of red blood cells in E14 *Twist-2* null ribs but not in wt embryos (Figures 3De and 3Df). Thus, *Twist-2* inhibits osteoblast differentiation in skeletal elements ossifying through intramembranous (clavicles) or endochondral mechanism (ribs).

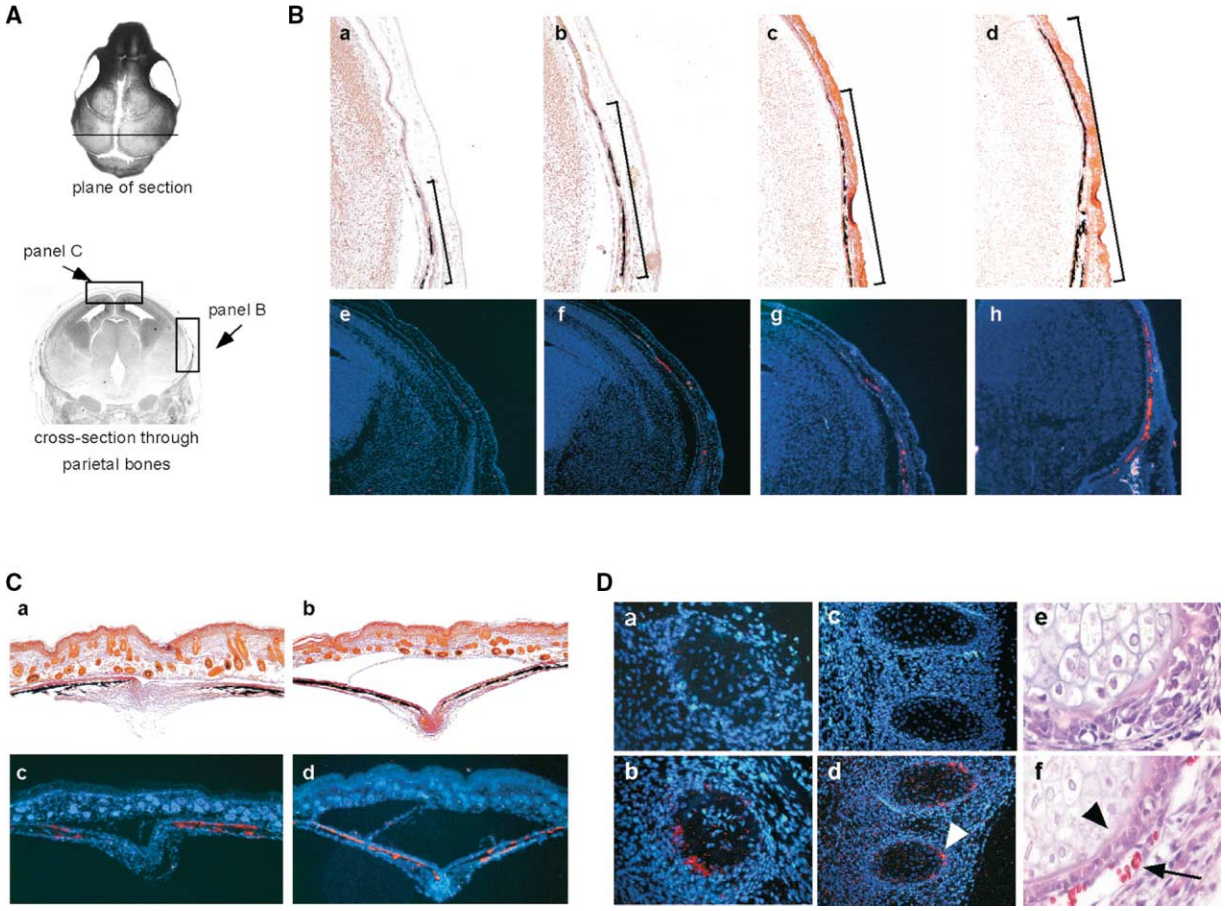


Figure 3. Twist-1 or Twist-2 Inhibits Osteoblast Differentiation

(A) Schematic illustration of the skull plans of section.

(B) Equivalent sections of E15 (Ba, Bb, Be, and Bf) and E16 skulls (Bc, Bd, Bg, and Bh) from wt (Ba, Bc, Be, and Bg) and *Twist-1*$^{+/-}$ (Bb, Bd, Bf, and Bh) embryos were analyzed for mineralized bone by von Kossa staining (Ba–Bd) and *Osteocalcin* expression (Be–Bh). E15 and E16 *Twist-1*$^{+/-}$ skulls had a broader area of mineralized trabeculae and more *Osteocalcin*-expressing cells than wt skulls. Brackets encompass areas of mineralized bone. Magnification: 100-fold, (Ba)–(Bd); 50-fold, (Be)–(Bh).

(C) Equivalent sections of P2 wt (Ca and Cc) and *Twist-1*$^{+/-}$ (Cb and Cd) skulls analyzed as above. *Twist-1*$^{+/-}$ skulls show a broader zone of mineralized bone and of *Osteocalcin*-expressing cells. Magnification: 100-fold, (Ca)–(Cd).

(D) Equivalent sections of E14 wt (Da and Dc) and *Twist-2* null (Db and Dd) embryos were analyzed for *Osteocalcin* expression. *Osteocalcin* was expressed in clavicles (Db) and ribs (Dd) of *Twist-2* null but not of wt embryos. Hematoxylin and eosin staining of E14 wt (De) or *Twist-2* null (Df) ribs. Note the presence of cuboidal osteoblast-like shape of the *Osteocalcin*-expressing cells (arrowhead). The presence of red blood cells (arrow) indicates initiation of vascular invasion in these skeletal elements. Magnification: 400-fold, (Da) and (Db); 200-fold, (Dc) and (Dd); and 800-fold, (De) and (Df).

### *Twist-1* Inhibits Osteoblast Differentiation without Affecting *Runx2* Expression

Next, we asked whether Twist proteins affect osteoblast differentiation with or without affecting *Runx2* expression. We first analyzed Runx2 expression in *Twist-1*$^{+/-}$ embryos and failed to detect any difference in the expression of this gene between mutant and wild-type embryos at all time points analyzed (Figure 4A). Next, we permanently transfected ROS 17/2.8 osteoblastic cells with *Twist-1* expression vectors. ROS 17/2.8 cells express genes characteristic of osteoblast progenitors, such as *Type I collagen* and *Tissue nonspecific alkaline phosphatase* (*Tnap*), and genes that define the differentiated osteoblast phenotype, such as *Osteocalcin*, an osteoblast-specific gene whose expression is regulated by Runx2 (Ducy et al., 1997). *Osteocalcin* expression was decreased in *Twist-1*-overexpressing ROS 17/2.8 cells, while expression of $\alpha$*1(I) Collagen* and *Tnap* was not affected (Figure 4B). This gene expression profile is reminiscent of the one observed in mesenchymal cells not yet committed to the osteoblast lineage (Aubin and Triffitt, 2002). Importantly, *Runx2* expression was not affected in *Twist-1*-overexpressing ROS 17/2.8 cells (Figure 4B). Overexpression of a deletion mutant of *Twist-1* lacking bHLH and C-terminal domains, $N_{Twist}$, did not affect osteoblast gene expression in ROS 17/2.8 cells, indicating that the N terminus of Twist-1 has no antiosteogenic function (Figure 4B). Conversely, in osteoblasts isolated from *Twist-1*$^{+/-}$ calvariae, there was an increase in expression of *Osteocalcin* and *Bsp*, a gene not expressed in ROS 17/2.8 cells, while expression of *Tnap*, $\alpha$*1(I) Collagen*, and *Runx2* was not modified (Figure 4C). This pattern of expression is a mirror image of the one described in *Twist-1*-overexpressing ROS 17/

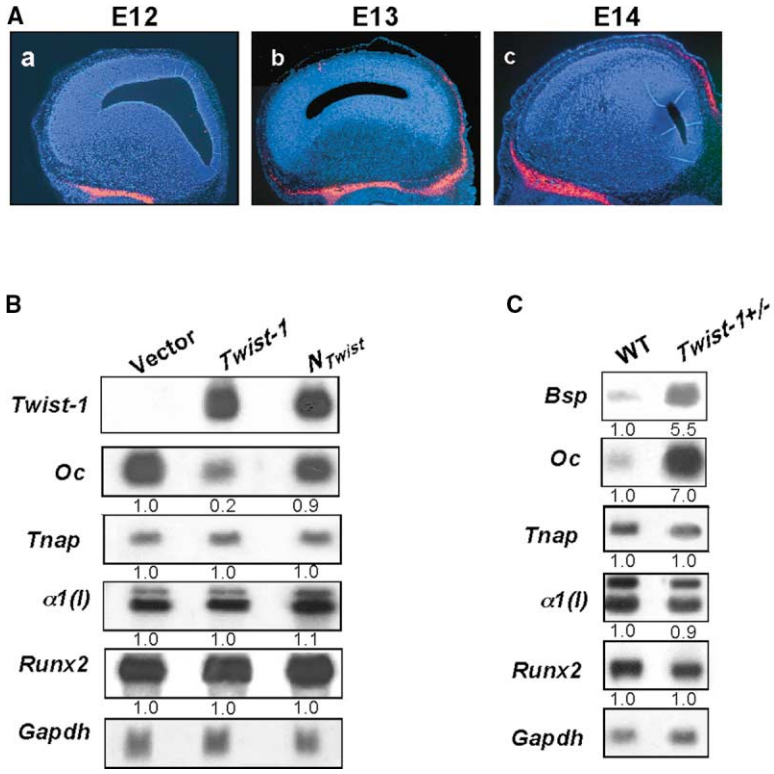


Figure 4. Inhibition of Osteoblast Differentiation with Normal *Runx2* Expression

(A) In situ hybridization showing unchanged *Runx2* expression in E12 (Aa), E13 (Ab), and E14 (Ac) *Twist-1*$^{+/-}$ embryos compared to wt embryos (compare to Figures 1A, 1D, and 1G).

(B) Northern blot analysis of total RNA isolated from ROS 17/2.8 cells permanently transfected with empty vector, *Twist-1*, or $N_{Twist}$ expression vectors. The blot was sequentially hybridized with probes for *Twist-1*, *Osteocalcin*, *Tnap*, *α1(I) Collagen*, *Runx2*, and *Gapdh* as a control. Note the decreased *Osteocalcin* expression in *Twist-1*-expressing but not in $N_{Twist}$-expressing cells. *Tnap*, *α1(I) Collagen*, and *Runx2* expression were not affected.

(C) Northern blot analysis of RNA isolated from *Twist-1*$^{+/-}$ or wt calvarial cells. *Twist-1*$^{+/-}$ cells show increase in *Osteocalcin* and *Bsp* without affecting *Runx2* expression.

2.8 cells. Taken together, these two experiments indicate that Twist-1 affects osteoblast differentiation as defined by osteoblast-specific gene expression without affecting *Runx2* expression. Additionally, the analysis of *Twist-1*$^{+/-}$ cells further supports the contention that inhibition of osteoblast differentiation by Twist-1 does not require the presence of chondrocytes, since osteoblasts in the skull appear through an intramembranous mechanism.

## Twist Proteins Inhibit Runx2 Transactivation Function

To determine whether Twist proteins inhibit osteoblast differentiation by inhibiting Runx2 function, we performed DNA cotransfection experiments in COS7 cells that do not express *Twist-1* or *-2*, *Runx2*, or any osteoblast-specific gene (data not shown). Transfection of a *Runx2* expression vector increased 100-fold the activity of an artificial promoter containing six Runx2 binding sites upstream of a luciferase (Luc) gene (p6OSE2-Luc) (Figure 5A). Introduction of *Twist-1* or *-2* expression vectors in this assay decreased Runx2-dependent Luc activity by 80% (Figure 5A). The inhibitory effect of Twist-1 on Runx2 transactivation function occurred in a dose-dependent manner (Figure 5B). Twist-1 could also inhibit Runx2 function when using the native *Osteocalcin* promoter-Luc chimeric gene (Figure 5C). Twist protein inhibition of Runx2 transactivation function was specific, since neither a zinc finger protein (Sp1) nor a leucine zipper protein (CREB) affected Runx2 transactivation function in this assay (Figure 5A). Conversely, Twist-1 did not affect Sp1's or CREB's ability to transactivate their respective reporter constructs (Figure 5D).

## The Twist Box as an Antiosteogenic Domain

To identify the domains within Twist proteins responsible for the inhibition of Runx2 function, we used Twist-1 deletion mutants in DNA cotransfection assays. All deletion mutants contained Twist-1's N terminus ($N_{Twist}$), a domain that has no detectable effect on osteoblast gene expression (Figures 4B) but that comprises Twist-1's nuclear localization signal (NLS) (Hamamori et al., 1999). $NB_{Twist}$, containing Twist-1's basic domain, failed to inhibit Runx2 transactivating function (Figure 5E). Likewise, $NBH_{Twist}$, a Twist-1 molecule containing the entire bHLH domain, did not affect Runx2's transactivation function (Figure 5E). A single amino acid substitution Twist-1 mutant that has lost its ability to heterodimerize, $H2Pro_{Twist}$ (Spicer et al., 1996), still inhibited Runx2-transactivating function. These experiments establish that Twist-1 bHLH domain is dispensable for the antiosteogenic function of this protein. In contrast, $NC_{Twist}$, a deletion mutant containing only Twist-1's N and C termini, inhibited Runx2 transactivating function even more efficiently than wt Twist-1, indicating that the antiosteogenic function of Twist-1 resides in its C terminus (Figure 5E). Further deletions revealed that Twist-1's antiosteogenic function is comprised in the sequence from amino acids 186 to 206 (Figure 5E). This domain is conserved in Twist-2, and Twist-1 and -2 are the only proteins containing this sequence. We called this antiosteogenic domain the Twist box (Figure 6A).

We also searched for Runx2 domains interacting with Twist proteins. All deletion mutants of Runx2 used in DNA transfection and immunoprecipitation experiments contained Runx2's NLS (Thirunavukkarasu et al., 1998). To test whether the DNA binding domain, or Runt domain, of Runx2 interacts with Twist proteins, we used

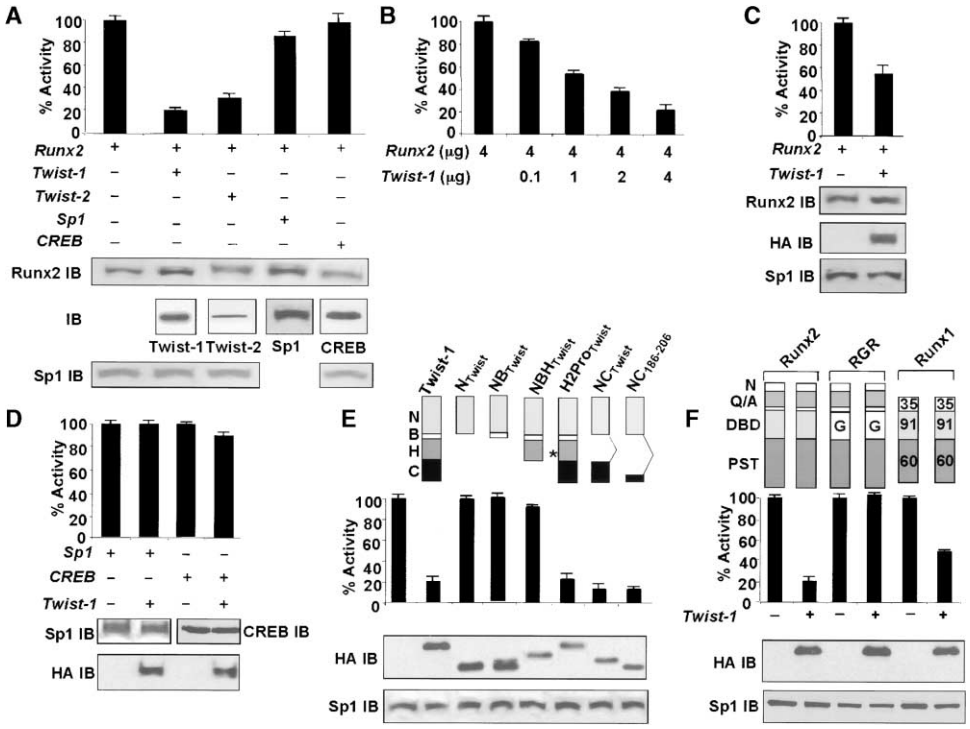


Figure 5. Twist-1 and -2 Inhibit Runx2 Transactivation Activity

(A–F) DNA cotransfection experiments. (A) p6OSE2-Luc reporter construct and *Runx2* expression vector were transiently cotransfected alone or with expression vectors for HA-*Twist-1, HA-Twist-2*, *Sp1*, or *CREB*. Twist proteins inhibited Runx2 transactivation function, while Sp1 and CREB did not. (B) p6OSE2-Luc reporter construct and *Runx2* expression vector were transiently cotransfected with different amounts of HA-*Twist-1* expression vector. Twist-1 inhibited Runx2 transactivation in a dose-dependent manner. (C) pOG2-reporter construct containing only one OSE2 site and a *Runx2* expression vector were transiently transfected with HA-*Twist-1*. Twist-1 inhibits Runx2 transactivation function when using a native OG2 promoter containing only one OSE2 site. (D) COS7 cells were transfected with either Sp1-responsive element-Luc or CREB-responsive element-Luc reporter constructs in the absence and presence of HA-*Twist*-1 expression vector. Fold activity was measured in the absence of HA-*Twist-1* and set at 100%. Twist-1 did not decrease the transactivation activity of endogenous Sp1 or CREB on their respective Luc-reporter constructs. (E) p6OSE2-Luc reporter was transiently transfected along with *Runx2* expression vectors and the indicated expression vectors for HA-*Twist-1*. Above, schematic diagrams of Twist-1 and Twist-1 mutants. Full-length Twist, $NC_{Twist}$, and $NC_{186-206}$ inhibited Runx2 transactivating function. (F) p6OSE2-Luc reporter was transiently transfected along with *Runx2*, RGR, or *Runx1* and the expression vectors for *Twist-1*. Above, schematic diagrams of Runx2, RGR, and Runx1. Twist-1 did not inhibit the transactivation activity of RGR, in which the Runx2 DNA binding domain was replaced with Gal4 DNA binding domain. Twist-1 inhibited Runx1 transactivation activity. Numbers indicate percentage homology between Runx1 and Runx2 in the N-terminal, Runt, and C-terminal domains. Lower panels in (A) and (C)–(F), Western blots of nuclear extracts from transfected cells showing the expression of the desired proteins. Values were expressed as percentage of the activity of 6OSE2-Luc or OG2-Luc with *Runx2* alone.

a UAS-reporter gene and a chimeric protein (RGR), in which Runx2's DNA binding domain was replaced by a Gal4 DNA binding domain (Lorch and Kornberg, 1985). RGR transactivated the UAS-Luc vector, but Twist-1 could not abrogate this transactivating function, strongly suggesting that the Runt domain interacts with Twist proteins (Figure 5F). To assess whether other domains of Runx2 were targets of Twist-1's antiosteogenic function, we replaced Runx2 in this assay with Runx1, a member of the Runx family that shares high homology with Runx2 only in its Runt domain (Bae et al., 1993). Twist-1 decreased Runx1 transactivation activity nearly as well as it affected Runx2 function (Figure 5F). These results indicate that the Runt domain is the main if not only domain in Runx2 interacting with the Twist box present in both Twist proteins.

## Inhibition of Runx2 DNA Binding Function by the Twist Box

To determine whether Twist proteins and Runx2 interact physically, COS7 cells were transfected with HA-tagged Twist-1 or -2 or Twist-1-deletion mutants and Flag-tagged Runx2 or Runx2-deletion mutants, nuclear extracts prepared, and immunoprecipitations performed. As suggested by the DNA cotransfections, Runx2 immunoprecipitated Twist-1 and -2. It also immunoprecipitated $NC_{Twist}$ and $NC_{186-206}$ but not $N_{Twist}$, $NB_{Twist}$, or $NBH_{Twist}$ (Figure 6B, left panel). Conversely, Twist-1 and $NC_{186-206}$ immunoprecipitated Runx2 and its Runt domain but did not immunoprecipitate NQA, a Runx2 deletion mutant containing its N-terminal and QA domains, or PST, containing only the C-terminal PST domain (Figure 6B, middle and right panels). These experiments establish that, in the conditions of this assay, the Runt domain is an essential part and perhaps the only domain of Runx2 interacting with the Twist box. This interaction could occur in vivo as endogenous Runx2 immunoprecipitated Twist-1 and endogenous Twist-1 immunoprecipitated Runx2 in osteoblasts (Figure 6C). Last, in a cell-free system, GST-Runx2 but not GST-CREB pulled down His-Twist-1, establishing that Twist-1 and Runx2 can interact directly (Figure 6D). In control experiments,

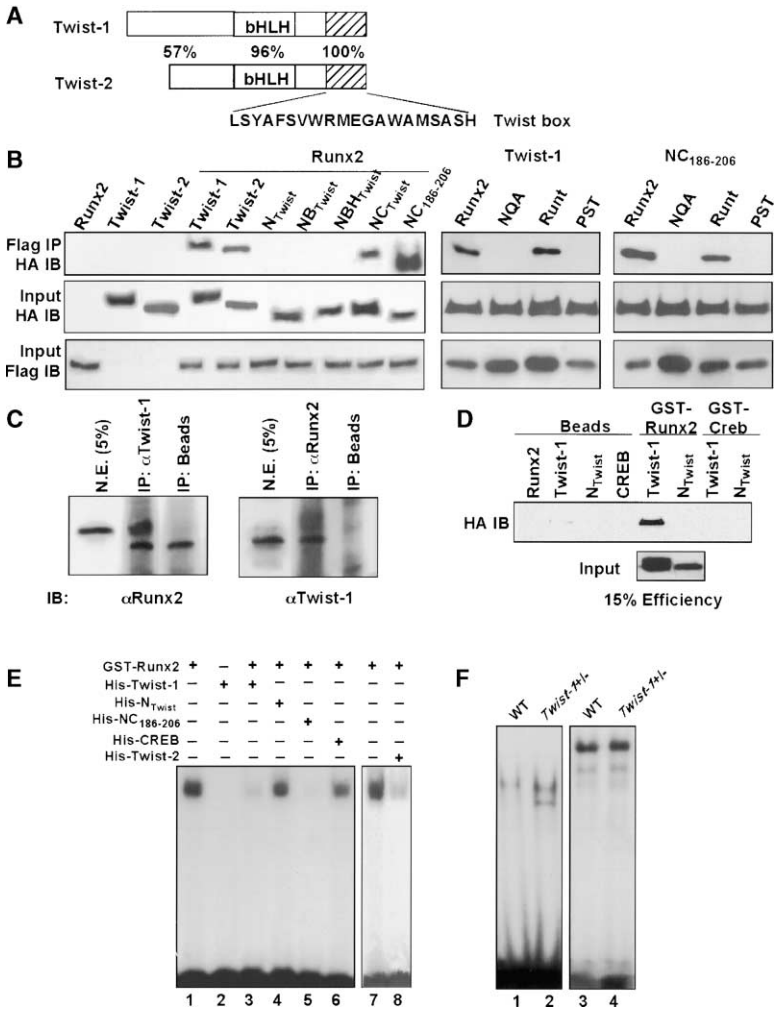


Figure 6. Identification of Twists' Antiosteogenic Domain

(A) Immunoprecipitation assays. COS7 cells were transiently transfected with expression vectors for Flag-*Runx2*, deletion mutants of Flag-*Runx2*, HA-*Twist-1*, HA-*Twist-2*, and deletion mutants of HA-*Twist-1*. Nuclear extracts were immunoprecipitated with anti-Flag antibody and then immunoblotted with anti-HA antibody. Twist-1 molecules containing the last 20 amino acid C-terminal domain interacted specifically with the DNA binding domain of Runx2. Below, 20 μg of input samples was immunoblotted with anti-Flag or anti-HA antibody.

(B) Runx2 interacted with Twist-1 in osteoblasts. Osteoblast nuclear extracts were immunoprecipitated with either anti-Twist-1 or anti-Runx2 antibodies and then analyzed by Western blot assays using anti-Runx2 or anti-Twist-1 antibodies. As controls, nuclear extracts were also incubated with Protein A Sepharose alone.

(C) Pull-down assays. GST-Runx2, GST-CREB, or buffer alone were incubated with His-Twist-1 or His-$N_{Twist}$ and then incubated with glutathione beads. Eluates from the beads were immunoblotted with anti-HA antibody. Only GST-Runx2 and His-Twist-1 showed direct interaction. Efficiency was determined by quantification of the amount of Twist-1 bound to the beads corrected by the amount of Runx2 bound.

(D) Gel retardation assay. Recombinant GST-Runx2 and His-Twist-1 (lane 3), His-$N_{Twist}$ (lane 4), His-$NC_{186-206}$ (lane 5), or His-CREB (lane 6) was incubated with labeled OSE2 oligonucleotides. His-Twist-1 and His-$NC_{186-206}$ decreased Runx2 DNA binding, while His-$N_{Twist}$ and His-CREB did not.

(E) Gel retardation assay. Nuclear extracts isolated from wt (lanes 1 and 3) and *Twist-1*$^{+/-}$ calvarial cells (lanes 2 and 4) were incubated with either labeled OSE2 (lanes 1 and 2) or Sp1 oligonucleotides (lanes 3 and 4). *Twist-1*$^{+/-}$ cells demonstrated increased Runx2 binding compared to wt while Sp1 binding to an Sp1 oligonucleotide appeared equal.

Twist did not immunoprecipitate Osx, Sp1, or CREB (data not shown).

The ability of Twist proteins to interact with Runx2's Runt domain implied that they should inhibit Runx2 DNA binding function. In gel retardation assays, Twist-1 and -2 markedly decreased binding of Runx2 to its cognate binding site, while $N_{Twist}$ did not. $NC_{186-206}$ was even more efficient than Twist-1 in preventing Runx2 from binding to DNA (Figure 6E, lanes 1–5). This inhibition was specific, as CREB did not inhibit Runx2's binding to DNA. Conversely, Twist-1 did not inhibit CREB binding to DNA (Figure 6E, lane 6, and data not shown). In the reverse experiment, nuclear extracts of *Twist-1*$^{+/-}$ osteoblasts showed increased binding ability to the Runx2 binding site but not to an Sp1 binding site (Figure 6F). Thus, the physical interaction between the Twist box of Twist proteins and the Runx2 Runt domain decreases Runx2's ability to bind to DNA and thereby its transactivation ability.

### In Vivo Mutagenesis of the Twist Box Leads to Premature Osteoblast Differentiation

We next tried to obtain in vivo confirmation of the Twist box function. A mouse mutant strain called Charlie Chaplin (*CC*/+), obtained through a screen for N-ethyl-N-nitrosourea (ENU)-induced dominant mutations (Justice, 2000), harbored a hindlimb polydactyly. Molecularly, the *CC* mutation is caused by a single amino acid substitution mutation (Ser192Pro) in the Twist box of Twist-1 (Figure 7A). In an immunoprecipitation assay, CC mutant protein interacted poorly with Runx2 (Figure 7B). Moreover, *CC*/+ mice have a craniosysnostosis phenotype with irregular lamboidal and coronal suture lines (Figure 6C). This skeletal phenotype and the biochemical data established that the *CC*/+ mutation is a loss-of-function allele for Twist box function. We then generated *CC/CC* mice that died immediately after birth. At E16, *CC/CC* displayed short limbs and polydactyly of the hindlimbs but no overt neural tube defect (data not shown). This contrasts with what was observed following deletion of the entire gene (Chen and Behringer, 1995).

To determine the role of serine 192 in osteoblast differentiation, we performed histological and gene expression analysis using *Osteocalcin* as a marker of differentiated osteoblasts in wt and *CC/CC* embryos from E14 to E18. Histological analysis of E14 *CC/CC* ribs showed no obvious differences compared to wt embryos. At E15, however, a thicker bone collar was consistently

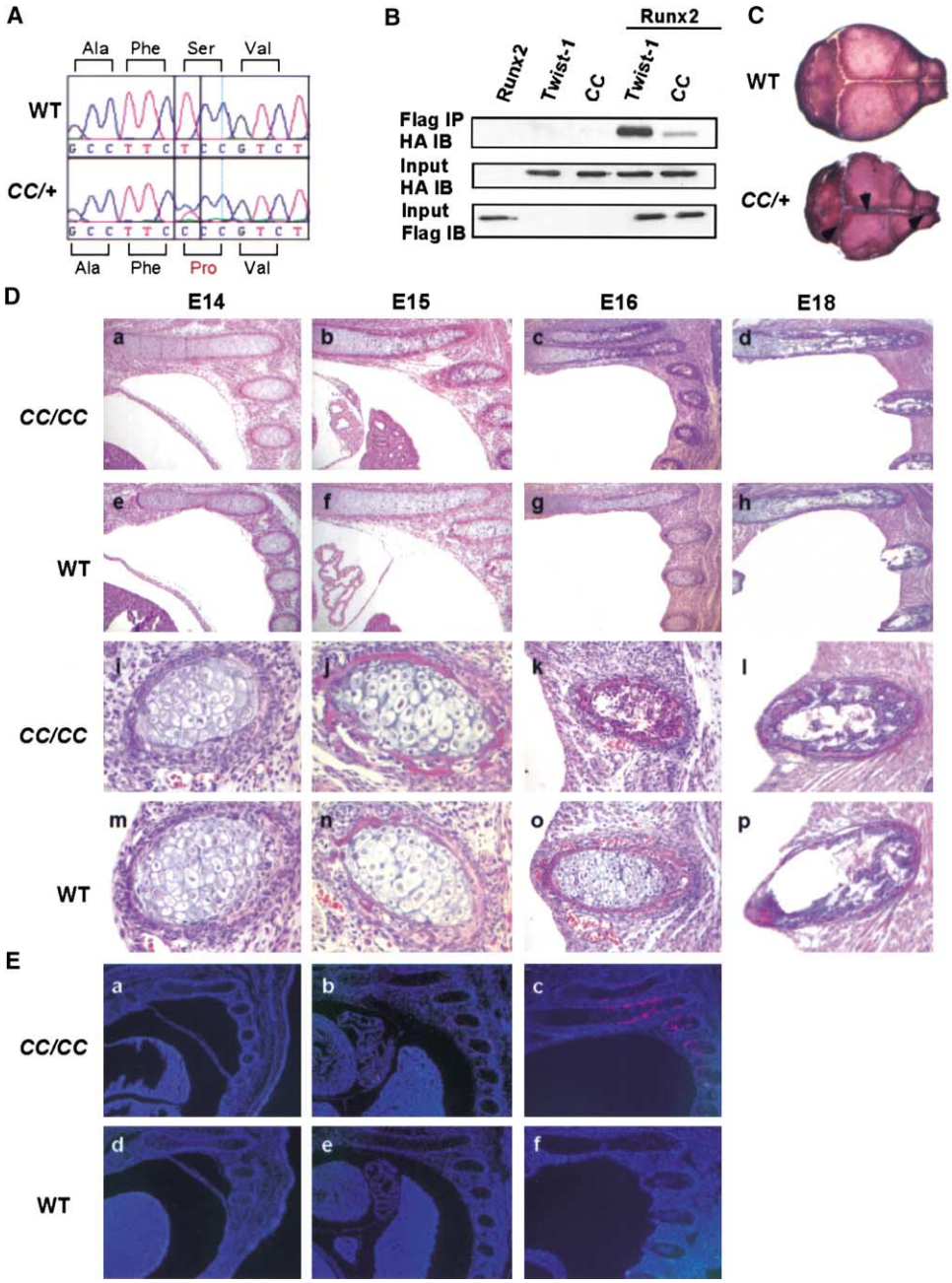


Figure 7. In Vivo Mutagenesis of the Twist Box

(A) Genomic sequencing of wt and Charlie Chaplin heterozygote (*CC/+*) *Twist-1* alleles showing a T → C base-pair change in *CC/+ Twist-1* resulting in a Ser192Pro mutation in the Twist box.

(B) Coimmunoprecipitation. COS7 cells were cotransfected with Flag-tagged *Runx2*, HA- tagged *Twist-1*, and a cc-*Twist-1* allele. Flag-Runx2 immunoprecipitated cc-Twist-1 poorly compared to Twist-1.

(C) Alcian blue/alizarin red staining of P10 skulls from wt and *CC/+* mice. Note the closed sutures in *CC/+* skulls (arrows).

(D) Histological analysis of E14 (Da, De, Di, and Dm), E15 (Db, Df, Dj, and Dn), E16 (Dc, Dg, Dk, and Do), and E18 ribs (Dd, Dh, Dl, and Dp) from wt (De–Dh and Dm–Dp) and *CC/CC* embryos (Da–Dd and Di–Dl). Note the presence of a thicker bone collar in E15 and E16 *CC/CC* compared to wt ribs. Note the presence of bone trabeculae in E16 *CC/CC* and E18 wt ribs. Magnification: 50-fold, (Dc), (Dd), (Dg), and (Dh); 100-fold, (Da), (Db), (De), and (Df); 200-fold, (Dk), (Dl), (Do), and (Dp); and 400-fold, (Di), (Dj), (Dm), and (Dn).

(E) In situ hybridization for *Osteocalcin* of E14 (Ea and Ed), E15 (Eb and Ee), and E16 (Ec and Ef) on equivalent sections from wt (Ed–Ef) and *CC/CC* (Ea–Ec) embryos. *Osteocalcin* is expressed as early as in E15 *CC/CC* ribs. Magnification: 50-fold, (Ea)–(Ef).

observed in *CC/CC* compared to wt ribs (Figures 7Db, 7Df, 7Dj, and 7Dn). Based on histological appearance, E15 *CC/CC* ribs looked more like E16 than E15 wt ribs. E16 *CC/CC* ribs were surrounded by a thick bone collar and contained in their center bone trabeculae, indicating that bone formation was advanced (Figures 7Dc and 7Dk). In comparable sections, the bone collar was consistently thinner, and there were no bone trabeculae in

the diaphysis of E16 wt ribs (Figures 7Dg and 7Do). At E18, wt and *CC/CC* ribs resembled each other, although *CC/CC* ribs had a thicker bone collar and consistently contained more trabeculae (Figures 7Dd, 7Dh, 7Dl, and 7Dp). Consistent with what was observed histologically, *Osteocalcin* expression could be detected as early as E15 in *CC/CC* ribs. In contrast, *Osteocalcin* expression was absent in wt E15 and 16 ribs (Figure 7E).

Since chondrocyte hypertrophy is a mandatory event preceding osteoblast differentiation, we analyzed chondrocyte differentiation in wt and *CC/CC* ribs from E14 to E18 using as molecular markers $\alpha$*1(II) collagen* for proliferating chondrocytes, *IndianHedgehog* (*Ihh*) for prehypertrophic chondrocytes, and $\alpha$*1(X) collagen* for hypertrophic chondrocytes. At E14, $\alpha$*1(II) collagen* and *Ihh* expression were virtually identical in wt and *CC/CC* ribs, and the same was true for these markers at all stages analyzed (Figures 8Aa–8Ap). In contrast, we observed a slight increase in $\alpha$*1(X) collagen* expression intensity in E14 *CC/CC* ribs compared to wt ribs, suggesting that chondrocyte hypertrophy was advanced in the mutant ribs. At E15, the same increase in $\alpha$*1(X) collagen* expression was noticeable in the *CC/CC* compared to wt ribs (Figures 8Ar and 8Av). At E16, $\alpha$*1(X) collagen* expression had increased noticeably in wt ribs, while it had markedly decreased in *CC/CC* ribs (Figures 8As and 8Aw). At E18, these three genes were not expressed anymore in wt and *CC/CC* ribs (Figures 8Ad, 8Ah, 8Al, 8Ao, 8As, and 8Ax). Thus, there is an acceleration of endochondral ossification in *CC/CC* ribs marked by a premature increase in $\alpha$*1(X) collagen* expression leading the way to premature osteoblast differentiation.

The advance in chondrocyte hypertrophy observed in *CC/CC* embryos led us to analyze *Twist-1* expression in wt developing ribs from E13 to E15. At those stages, *Twist-1* was expressed in *Runx2*- and subsequently *Bsp*-expressing cells of the perichondrium/bone collar but never above background level in presumptive chondrocytes in the center of the ribs (data not shown). This observation is in agreement with the notion that cells of the perichondrium inhibit chondrocyte hypertrophy, a process itself dependent in part on *Runx-2* expression (Long and Linsenmayer, 1998; Di Nino et al., 2001; Takeda et al., 2001; Ueta et al., 2001), and indicates that Twist-1 is a mediator of this negative regulation of the later phases of endochondral ossification.

## Discussion

This study reveals that osteoblast differentiation is a negatively regulated process early during skeletogenesis, despite a normal expression of *Runx2* (Figure 8B). The interaction between Runx2's DNA binding domain and the Twist box, a newly identified antiosteogenic domain present in the two Twist proteins, provides the molecular basis for this inhibition. Eventually, the decrease of *Twist* genes' expression triggers osteoblast differentiation defined by expression of genes downstream of Runx2. This study demonstrates also that the molecular defect in Saethre-Chotzen syndrome, a skeletal dysplasia caused by haploinsufficiency at the *TWIST* locus, is a premature activity of Runx2.

### The Twist Box as an Antiosteogenic Domain

Several lines of evidence indicate that Twist proteins inhibit osteoblast differentiation by interfering with Runx2 function. First, expression of molecular markers of differentiated osteoblasts in *Runx2*-expressing cells is not detectable as long as *Twist* genes are expressed in these cells. Second, mice heterozygotes for *Twist-1* and *Runx2* deletions have a normal skull, and double mutants for *Twist-2* and *Runx2* have normal clavicles. Third, Twist proteins and Runx2 physically interact, and this interaction affects Runx2 DNA binding function. Molecular and genetic evidence establishes that Twists' antiosteogenic function is exerted by a 20 amino acid-long domain, the Twist box, a domain distinct from their bHLH domains. In vitro, only the Twist-1 deletion mutants that contain the Twist box interact with Runx2. In cell culture, a deletion mutant of Twist-1 containing its N-terminal domain and the Twist box inhibited Runx2 transactivating function, and a single amino acid substitution in the Twist box of Twist-1 results in premature osteoblast differentiation in vivo. Interestingly, the Twist box is more highly conserved in vertebrates than in invertebrates (Castanon and Baylies, 2002).

### Twist Box and Saethre-Chotzen Syndrome

Although there is no mutational hot spot in *Twist-1* (Gripp et al., 2000), nearly half of the mutations result in premature termination before the Twist-1 C-terminal domain or are frameshift mutations. The absence of any Twist box in this class of mutation could easily explain the occurence of the disease. Another group of Saethre-Chotzen mutations are missense mutations that do not affect the Twist-1 C terminus. The existence of this type of mutation, along with recent studies using transformed cells obtained from a Saethre-Chotzen patient and showing an increase in *Osteocalcin* expression (Elanko et al., 2001), suggests that more than one mechanism may be at work to cause Saethre-Chotzen Syndrome. However, the contention that the antiosteogenic function of the Twist box is conserved in human is supported by the fact that human Runx2 and human Twist-1 can interact physically (see Supplemental Figure S1B at http://www.developmentalcell.com/cgi/content/full/6/3/423/DC1) and by the existence of a Saethre-Chotzen-causing mutation that leaves intact Twist-1's bHLH domain but removes its Twist box (Gripp et al., 2000). Interestingly, this mutation causes a more severe form of the disease, with limb patterning defects similar to the ones observed in *CC/CC* mice.

### The Twist Code as the Earliest Regulator of Osteoblast Differentiation

Histologic and gene expression analyses of *Twist-1*- and *-2*-deficient and *CC/CC* embryos establish that Twist proteins' antiosteogenic function affects bones ossifying either through an intramembranous or an endochondral process. Although no premature ossification outside the skull has been noted in *Twist-1*$^{+/-}$ embryos, one cannot exclude that a systematic analysis of *Osteocalcin* expression throughout the skeleton of these mutant mice may reveal premature osteoblast differentiation. That premature osteoblast differentiation takes place in the *CC/CC* embryos suggests that it is a

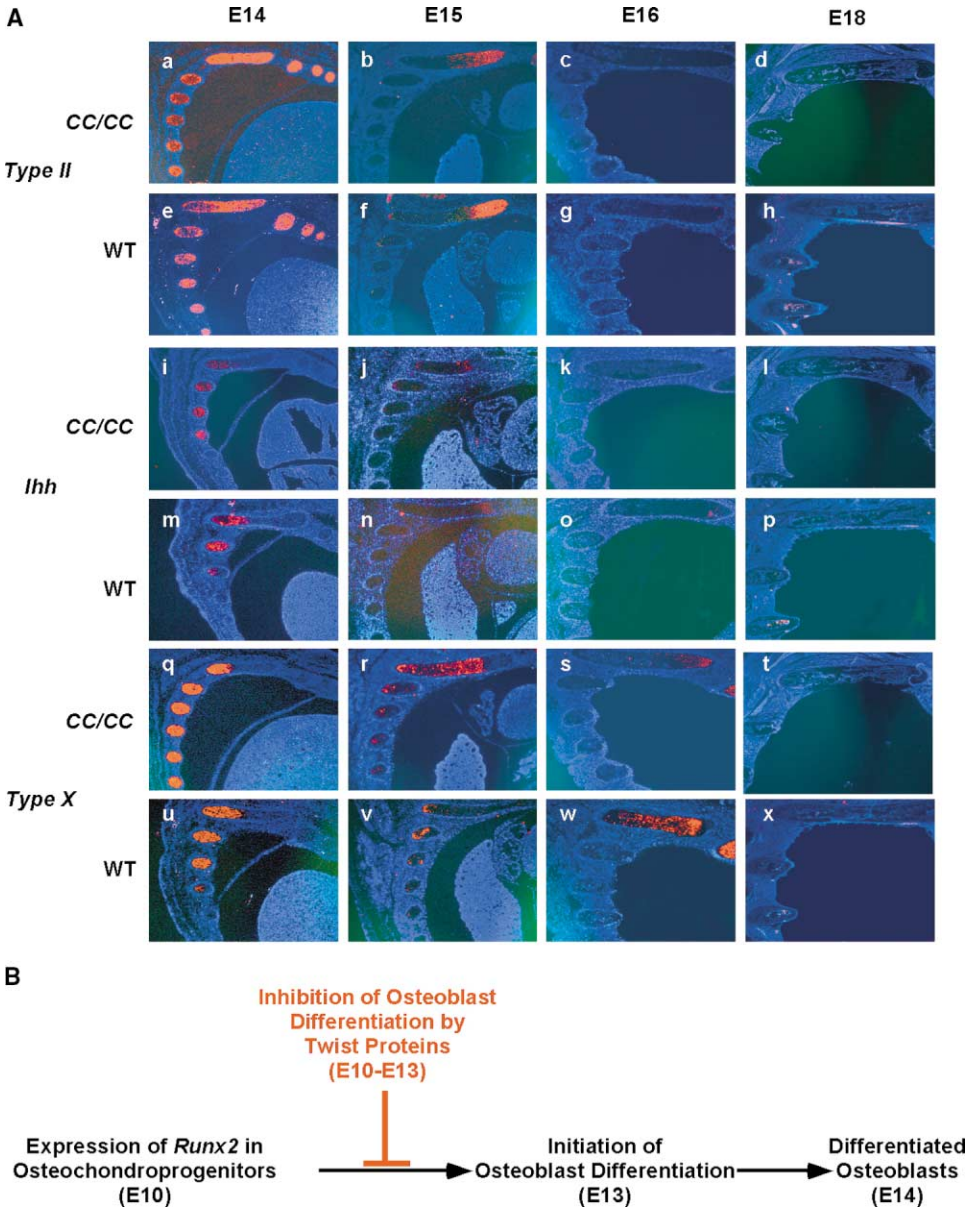


Figure 8. Chondrocyte Development in *CC/CC* Mice

(A) In situ hybridization for $\alpha$*1(II) collagen* (Aa–Ah), *Ihh* (Ai–Ap), and $\alpha$*1(X) collagen* (Aq–Ax) at E14 (Aa, Ae, Ai, Am, Aq, and Au), 15 (Ab, Af, Aj, An, Ar, and Av), 16 (Ac, Ag, Ak, Ao, As, and Aw), and 18 (Ad, Ah, Al, Ap, At, and Ax) in ribs of *CC/CC* (Aa–Ad, Ai–Al, and Aq–At) and wt embryos (Ae–Ah, Am–Ap, and Au–Ax). Normal $\alpha$*1(II) collagen* and *Ihh* expression while $\alpha$*1(X) collagen* is increased in E14 and E15 *CC/CC* ribs.

(B) A current model of osteoblast differentiation during development. Runx2 is the earliest identified factor required for osteoblast differentiation. Its function is, however, transiently inhibited by *Twists* whose decrease in expression determines when osteoblast differentiation can occur.

likely possibility. This negative regulation of osteoblast differentiation could also be achieved by Twist-1 together with Twist-2, since they are coexpressed in most developing skeletal elements. This could be tested by generating *CC/CC*; *Twist-2* null double mutant mice, provided they live. The fact that the Twist box is present only in Twist-1 and -2 indicates that only these two proteins can delay osteoblast differentiation early during development through the mechanism described here.

## Twist Functions and Twist Domains

The bHLH domain of Twist proteins is dispensable for their antiosteogenic function. It was recently shown that, after birth, Twist proteins inhibit NF-$\kappa$B activity by interacting with RelA and that this function is not mediated by their bHLH domains. Surprisingly, although this Twist-2 function also requires its C terminus, NF-$\kappa$B's DNA binding ability was not affected by Twist (Sosic et al., 2003). This lack of DNA binding inhibition contrasts with what we observed in the case of Runx2. At the present time, the molecular basis for this difference in the mode of action of Twist is not fully understood. Ectopic expression of *Twist-1* in cell culture experiments inhibits muscle gene expression (Hebrok et al., 1994; Spicer et al., 1996), and Twist-1 can inhibit MyoD's DNA binding ability and Mef2's transactivating function in vitro. Unlike

that which is the case for its antiosteogenic actions or its inhibition of NF-κB, this Twist antimyogenic function requires both its bHLH and C terminus domains (Spicer et al., 1996). These findings and our results suggest that different functions exerted by the Twist proteins may use the same domains of the proteins. Further in vivo-directed mutagenesis will allow us to address the respective role of each domain of the Twist proteins in their various functions and, in particular, which functions are controlled by the Twist box.

## Experimental Procedures

### Mutant Animals

*Twist-1-* and *Twist-2*-deficient mice have been described (Chen and Behringer, 1995; Sosic et al., 2003). Genotyping was performed by PCR analysis of genomic DNA. The Charlie Chaplin (CC) mutation arose in the first generation offspring of ENU-treated males. Eight-week-old C57BL/6J males were injected intraperitoneally (100 mg ENU/kg) weekly for 3 weeks. The polydactyly phenotype of *CC*/+ was observed in 1 of 905 G1 animals produced from these treated males. Subsequent breeding confirmed dominant inheritance, as 52 of 108 animals had extra digits on both hindlimbs.

### Skeletal Preparations, Histology, In Situ Hybridization, and Immunohistochemistry

For skeletal preparations, mice were dissected, fixed in 95% ethanol, and stained in alcian blue and alizarin red according to standard protocols (McLeod, 1980). Analysis of intraparietal bones was made using calipers. At least six mice were analyzed per genotype. For histology, samples were fixed in 4% paraformaldehyde/PBS overnight at 4°C, processed for paraffin embedding, and sectioned at 5 μm. Sections were stained with hematoxylin and eosin or von Kossa and counterstained by van Gieson. In situ hybridization was performed using $^{35}$S-labeled riboprobes. Hybridizations were performed at 60°C. Autoradiography and Hoechst 33258 staining were performed as described (Takeda et al., 2001). HA-Twist-1 was detected with a goat anti-HA antibody (Roche) (1:1000) using ABC Elite Kit (Vector) and NovaRed (Vector) as a substrate.

### RNA Analysis and DNA Transfection Experiments

Total RNA was isolated from the indicated sources and Northern blot analysis performed using standard protocols and previously described probes (Ducy et al., 1997). RT-PCR analysis was performed using DNaseI-treated total RNA. For DNA transfections, COS7 and ROS 17/2.8 cells were grown in DMEM and DMEM-F12, respectively, both with 10% FBS. Calcium-phosphate precipitation was used for transient DNA transfections. Four micrograms of reporter and indicated quantities of expression plasmids were transfected along with 1 μg of RSV-β-galactosidase to control for transfection efficiency. Assays were performed and extracts isolated as previously described (Ducy et al., 1997). For permanent transfections, cells were selected using 400 μg/ml G418 and clones harvested individually and amplified under selection prior to analysis. Southern blot analysis verified the presence of the appropriate transgene in each clone analyzed.

### Protein Chemistry and DNA Binding Assay

#### *Immunoprecipitations*

Five hundred micrograms of nuclear extracts of COS7 cells transfected with indicated expression constructs were incubated with anti-Flag beads (Sigma-Aldrich) for 2 hr in 500 μl of NTN buffer (200 mM NaCl, 50 mM Tris [pH 8.0], 0.5% NP-40) at 4°C with rotation. Beads were washed four times with NTN buffer and boiled in SDS-PAGE loading buffer. Eluates were subjected to SDS-PAGE and immunoblotted using the indicated antibody.

#### *Western Blot Analysis*

Blots were immunolabeled with rabbit anti-HA (Santa Cruz Biotechnology; 1:2000), rabbit anti-Runx2 (Sigma; 1:3000), or mouse anti-Flag (Sigma-Aldrich; 1:2000) followed by secondary labeling with goat anti-rabbit or rabbit anti-mouse HRP-conjugated antibodies (1:2000) and luminol detection.

#### *Recombinant Proteins*

GST-fusion proteins were isolated from bacterial lysate using glutathione beads, and His-tagged proteins were isolated from bacterial lysate using the Talon system (Clontech) according to manufacturers' directions.

#### *Pull-Down Assays*

Fifty micrograms of GST-fusion protein was incubated with 400 μg His-tagged protein and glutathione beads. The beads were then washed three times and boiled in SDS-PAGE loading buffer. Eluates were subjected to SDS-PAGE, transferred to nitrocellulose membrane, and immunoblotted using appropriate antibody. Efficiency was calculated by comparing known amounts of GST-Runx2 and His-Twist to eluted GST-Runx2 and His-Twist-1 followed by correcting the percentage of His-Twist-1 bound to the beads by the amount of GST-Runx2 bound. For gel retardation assay (GRA), labeled double-stranded oligonucleotides were prepared and GRA performed as described (Ducy and Karsenty, 1995), and His-Twist proteins were added to the GRA reaction and incubated on ice for 30 min prior to loading onto a 5% acrylamide gel.

## Acknowledgments

We thank R. Behringer and P. Tam for kindly providing *Twist-1*-deficient mice; S. Takeda and M. Tetzlaff for technical assistance; and P. Ducy for critical reading of the manuscript. This work was supported by the National Institutes of Health (to G.K., D.M.O., E.N.O. M.J.J., and B.K.), the Arthritis Foundation (P.B.), the Children's Brittle Bone Foundation (X.Y.), and an Eli Lilly Research Agreement (G.K.).

Received: June 27, 2003
Revised: January 9, 2004
Accepted: January 12, 2004
Published: March 15, 2004

## References

Aubin, J.E., and Triffitt, J.T. (2002). Messenchymal Stem Cells and Osteoblat Differentiation, Volume 1, Second Edition (San Diego, CA: Academic Press).

Bae, S.C., Yamaguchi-Iwai, Y., Ogawa, E., Maruyama, M., Inuzuka, M., Kagoshima, H., Shigesada, K., Satake, M., and Ito, Y. (1993). Isolation of PEBP2 alpha B cDNA representing the mouse homolog of human acute myeloid leukemia gene, AML1. Oncogene *8*, 809–814.

Bianco, P., Fisher, L.W., Young, M.F., Termine, J.D., and Robey, P.G. (1991). Expression of bone sialoprotein (BSP) in developing human tissues. Calcif. Tissue Int. *49*, 421–426.

Castanon, I., and Baylies, M.K. (2002). A Twist in fate: evolutionary comparison of Twist structure and function. Gene *287*, 11–22.

Chen, J., Shapiro, H.S., and Sodek, J. (1992). Development expression of bone sialoprotein mRNA in rat mineralized connective tissues. J. Bone Miner. Res. *7*, 987–997.

Chen, Z.F., and Behringer, R. (1995). Twist is required in head mesenchyme for cranial neural tube morphogenesis. Genes Dev. *9*, 686–699.

Di Nino, D.L., Long, F., and Linsenmayer, T.F. (2001). Regulation of endochondral cartilage growth in the developing avian limb: cooperative involvement of perichondrium and periosteum. Dev. Biol. *240*, 433–442.

Ducy, P. (2000). Cbfa1: a molecular switch in osteoblast biology. Dev. Dyn. *19*, 461–471.

Ducy, P., and Karsenty, G. (1995). Two distinct osteoblast-specific cis-acting elements control expression of a mouse osteocalcin gene. Mol. Cell. Biol. *15*, 1858–1869.

Ducy, P., Zhang, R., Geoffroy, V., Ridall, A.L., and Karsenty, G. (1997). Osf2/Cbfa1: a transcriptional activator of osteoblast differentiation. Cell *89*, 747–754.

El Ghouzzi, V., Le Merrer, M., Perrin-Schmitt, F., Lajeunie, E., Benit, P., Renier, D., Bourgeois, P., Bolcato-Bellemin, A.L., Munnich, A.,

and Bonaventure, J. (1997). Mutations of the Twist gene in the Saethre-Chotzen syndrome. Nat. Genet. *15*, 42–46.

Elanko, N., Sibbring, J.S., Metcalfe, K.A., Clayton-Smith, J., Donnai, D., Temple, I.K., Wall, S.A., and Wilkie, A.O. (2001). A survey of TWIST for mutations in craniosynostosis reveals a variable length polyglycine tract in asymptomatic individuals. Hum. Mutat. *18*, 535–541.

Gripp, K.W., Zackai, E.H., and Stolle, C.A. (2000). Mutations in the human TWIST gene. Hum. Mutat. *15*, 479.

Hamamori, Y., Sartorelli, V., Ogryzko, V., Puri, P.L., Wu, H.Y., Wang, J.Y., Nakatani, Y., and Kedes, L. (1999). Regulation of histone acetyltransferases p300 and PCAF by the bHLH protein Twist and adenoviral oncoprotein E1A. Cell *96*, 405–413.

Hebrok, M., Wertz, K., and Fuchtbauer, E.M. (1994). M-twist is an inhibitor of muscle differentiation. Dev. Biol. *165*, 537–544.

Howard, T.M., Paznekas, W.A., Green, E.D., Chiang, L.C., Ma, N., Ortiz de Luna, R.I., Garcia Delgado, C., Gonzalez-Ramos, M., Kline, A.D., and Jabs, E.W. (1997). Mutations in Twist, a basic helix-loop-helix transcription factor, in Saethre-chotzen syndrome. Nat. Genet. *15*, 36–41.

Justice, M.J. (2000). Capitalizing on large-scale mouse mutagenesis screens. Nat. Rev. Genet. *1*, 109–115.

Karsenty, G., and Wagner, E.F. (2002). Reaching a genetic and molecular understanding of skeletal development. Dev. Cell *2*, 389–406.

Kaufman, J.M., Taelman, P., Vermeulen, A., and Vandeweghe, M. (1992). Bone mineral status in growth hormone-deficient males with isolated and multiple pituitary deficiencies of childhood onset. J. Clin. Endocrinol. Metab. *74*, 118–123.

Komori, T., Yagi, H., Nomura, S., Yamaguchi, A., Sasaki, K., Deguchi, K., Shimizu, Y., Bronson, R.T., Gao, Y.H., Inada, M., et al. (1997). Targeted disruption of Cbfa1 results in a complete lack of bone formation owing to maturational arrest of osteoblasts. Cell *89*, 755–764.

Li, L., Cserjesi, P., and Olson, E.N. (1995). Dermo-1: a novel twist-related bHLH protein expressed in the developing dermis. Dev. Biol. *172*, 280–292.

Long, F., and Linsenmayer, T.F. (1998). Regulation of growth region cartilage proliferation and differentiation by perichondrium. Development *125*, 1067–1073.

Lorch, Y., and Kornberg, R.D. (1985). A region flanking the GAL7 gene and a binding site for GAL4 protein as upstream activating sequences in yeast. J. Mol. Biol. *186*, 821–824.

McLeod, M.J. (1980). Differential staining of cartilage and bone in whole mouse fetuses by alcian blue and alizarin red S. Teratology *22*, 299–301.

Mundlos, S., and Olsen, B.R. (1997). Heritable diseases of the skeleton. Part I: Molecular insights into skeletal development-transcription factors and signaling pathways. FASEB J. *11*, 125–132.

Nakashima, K., Zhou, X., Kunkel, G., Zhang, Z., Deng, J.M., Behringer, R.R., and de Crombrugghe, B. (2002). The novel zinc finger-containing transcription factor osterix is required for osteoblast differentiation and bone formation. Cell *108*, 17–29.

Otto, F., Thornell, A.P., Crompton, T., Denzel, A., Gilmour, K.C., Rosewell, I.R., Stamp, G.W., Beddington, R.S., Mundlos, S., Olsen, B.R., et al. (1997). Cbfa1, a candidate gene for cleidocranial dysplasia syndrome, is essential for osteoblast differentiation and bone development. Cell *89*, 765–771.

Sosic, D., Richardson, J.A., Yu, K., Ornitz, D.M., and Olson, E.N. (2003). Twist regulates cytokine gene expression through a negative feedback loop that represses NF-kappaB activity. Cell *112*, 169–180.

Spicer, D.B., Rhee, J., Cheung, W.L., and Lassar, A.B. (1996). Inhibition of myogenic bHLH and MEF2 transcription factors by the bHLH protein Twist. Science *272*, 1476–1480.

Takeda, S., Bonnamy, J.P., Owen, M.J., Ducy, P., and Karsenty, G. (2001). Continuous expression of Cbfa1 in nonhypertrophic chondrocytes uncovers its ability to induce hypertrophic chondrocyte differentiation and partially rescues Cbfa1-deficient mice. Genes Dev. *15*, 467–481.

Thirunavukkarasu, K., Mahajan, M., McLarren, K.W., Stifani, S., and Karsenty, G. (1998). Two domains unique to osteoblast-specific transcription factor Osf2/Cbfa1 contribute to its transactivation function and its inability to heterodimerize with Cbfbeta. Mol. Cell. Biol. *18*, 4197–4208.

Ueta, C., Iwamoto, M., Kanatani, N., Yoshida, C., Liu, Y., Enomoto-Iwamoto, M., Ohmori, T., Enomoto, H., Nakata, K., Takada, K., et al. (2001). Skeletal malformations caused by overexpression of Cbfa1 or its dominant negative form in chondrocytes. J. Cell Biol. *153*, 87–100.

Wolf, C., Thisse, C., Stoetzel, C., Thisse, B., Gerlinger, P., and Perrin-Schmitt, F. (1991). The M-twist gene of Mus is expressed in subsets of mesodermal cells and is closely related to the Xenopus X-twi and the Drosophila twist genes. Dev. Biol. *143*, 363–373.